

Extended FF and V_{OC} Parameterizations for Silicon Solar Cells

Karsten Bothe , Member, IEEE, David Hinken , and Rolf Brendel 

Abstract—This work is concerned with maximal and currently obtained fill factors of crystalline silicon solar cells. Recent research activities have led to a drastically decreased recombination in the volume as well as at the surfaces and interfaces of crystalline silicon solar cells. As a result, open-circuit voltages (V_{OC}) and fill factor (FF) values increased significantly. In order to classify how good the achieved improvements are, it is necessary to know the maximum achievable values. Unfortunately, there is no explicit expression for the FF in terms of other characteristic solar cell parameters. For this reason, the empirical FF_0 -relation by Green is widely used to predict upper FF bounds for a given V_{OC} . In order to evaluate to what extent Green’s relation is a good approximation to recently obtained values, we study FF - V_{OC} relations for ideal resistance-free single junction silicon solar cells limited by intrinsic recombination using state-of-the-art analytical models. The obtained upper bounds are compared with recently published record values showing that all values stay below the intrinsic limit. We provide parameterizations of V_{OC} and FF as a function of sample thickness w and base dopant density N_{dop} .

Index Terms—Fill factor, open-circuit voltage, silicon, solar cell.

I. INTRODUCTION

THE progress in research and development of crystalline silicon solar cells over the past years has not only led to excellent passivated surfaces and interfaces [1] but also to lowly recombinative, passivating contacts [2]. The associated minimization of charge carrier recombination has led to considerably increased open-circuit voltages (V_{OC}) and high fill factors (FF). The data measured at the ISFH CalTeC Solar Cell Calibration Laboratory also shows a general trend toward higher FF - V_{OC} values within the past years. As shown in Fig. 1, fill factor values of up to 86.6% have been published recently [3].

The maximum achievable fill factor of a solar cell cannot be determined directly from other characteristic solar cell parameters. Thus, the well-known empirical relation

$$FF_0 = \frac{v_{OC} - \ln(v_{OC} - 0.72)}{v_{OC} + 1} \quad (1)$$

Manuscript received 2 June 2023; revised 16 August 2023; accepted 24 August 2023. Date of publication 14 September 2023; date of current version 7 November 2023. This work was supported by the State of Lower Saxony. (Corresponding author: Karsten Bothe.)

Karsten Bothe and David Hinken are with the Institut für Solarenergieforschung (ISFH), 31860 Emmerthal, Germany (e-mail: k.bothe@isfh.de; hinken@isfh.de).

Rolf Brendel is with the Institut für Solarenergieforschung (ISFH), 31860 Emmerthal, Germany, and also with the Institute for Solid State Physics, Leibniz Universität Hannover, 30167 Hannover, Germany (e-mail: brendel@isfh.de).

Color versions of one or more figures in this article are available at <https://doi.org/10.1109/JPHOTOV.2023.3309932>.

Digital Object Identifier 10.1109/JPHOTOV.2023.3309932

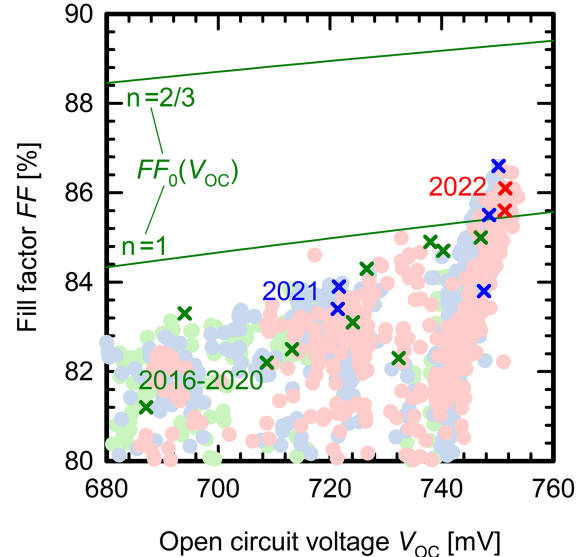


Fig. 1. Experimental FF - V_{OC} pairs of crystalline silicon solar cells and FF - V_{OC} relation (green lines) as predicted by Green’s equation using $n = 1$ and $2/3$, respectively. Experimental values shown as crosses are taken from the 55th to 61st editions of the solar cell efficiency tables. Experimental values shown as filled colored circles are the selected data from measurements carried out at the ISFH CalTeC Solar Cell Calibration Laboratory (red: Data from 2022, blue: Data from 2021, and green: Data from 2016 to 2020).

of Green [4], [5], with v_{OC} being the normalized open-circuit voltage $V_{OC}/(nkT/q)$ (n is the diode ideality factor, k is the Boltzmann factor, T is the temperature, and q is the elementary charge), is often used to evaluate the fill factor potential of a solar cell for a given open-circuit voltage.

To apply Green’s relation, one has to make an assumption for the ideality factor n . For simplicity and due to the fact that the correct value is usually unknown, a value of one is commonly assumed.

As an increasing number of values are above the FF - V_{OC} limit calculated by (1) with $n = 1$, there have been some discussions about the extent to which these values have been correctly determined. While the aspect of the metrological correct determination of fill factors has already been discussed extensively in the literature [6], [7], [8], we study FF - V_{OC} limits related to intrinsic recombination in silicon in this work.

In order to evaluate to what extent this simplification is a good approximation and under which conditions also higher FF values might be achieved experimentally, we perform analytical current-voltage (J - V) curve calculations for ideal

resistance-free solar cells limited by intrinsic recombination only. From the J - V curves, we calculate the corresponding FF - V_{OC} data pairs. By varying the base dopant density, the calculated FF - V_{OC} data pairs build up to an FF - V_{OC} curve, which we compare to the curves obtained from Green's relation for ideality factors of 1 and 2/3 corresponding to cells limited by radiative and Auger recombination, respectively. Since analytical solar cell simulations require an extensive understanding and knowledge of the numerous models and parameterizations they are based on, we provide suitable parameterizations for calculating upper bounds of the FF and V_{OC} as a function of the sample thickness w and the base dopant density N_{dop} . Using our simulations, we finally evaluate recently published high FF and V_{OC} values of high-efficiency solar cells.

II. ANALYTICAL CALCULATION OF J - V CURVES

We model the current–voltage (J - V) curve of single junction solar cells using

$$J(V) = J_{\text{gen}}(V) - J_{\text{rec}}(V) \quad (2)$$

with J being the current density, V the voltage, $J_{\text{gen}}(V)$ the light-generated current density, and $J_{\text{rec}}(V)$ the recombination current density. In order to allow for a comparison to experimental data usually determined at 25 °C, we also carry out all calculations at this temperature. The generation current J_{gen} is calculated as described in [9] by

$$J_{\text{gen}}(V) = \frac{q}{hc} \int A_{\text{BB}}(\lambda, w, V) E_{\text{AM1.5G}}(\lambda) d\lambda \quad (3)$$

with the band-to-band absorption A_{BB} expressed as

$$A_{\text{BB}}(\lambda, w, V) = \frac{\alpha_{\text{BB}}}{\alpha_{\text{BB}} + \alpha_{\text{FCA}}} \frac{(1 - T_r)(1 - T_r)n^2}{n^2 - (n^2 - 1)T_r^2}. \quad (4)$$

The coefficient of free carrier absorption α_{FCA} is calculated according to Rüdiger et al. [10] and T_r as described by Brendel [11]. For α_{BB} , we use the data from Green [12], [13].

Depending on the used references, the calculation of the recombination current density is based either on the excess charge carrier density or on the respective voltage. Both are connected according to

$$V = \frac{kT}{q} \log \left(\frac{(n_0 + \Delta n)(p_0 + \Delta p)}{n_{i,\text{eff}}^2} \right) \quad (5)$$

with

$$n_{i,\text{eff}} = n_{i0} \exp \left(\frac{q}{kT} \frac{\Delta E_g}{2} \right) \quad (6)$$

where n_{i0} is calculated according to the authors in [14] and [15]. The impact of band gap narrowing ΔE_g is taken into account as described by Schenk et al. [16], [17].

Aiming at calculating the upper FF and V_{OC} bounds, we only take into account intrinsic recombination. Consequently, J_{rec} is composed of the terms J_{rad} and J_{Auger} , which describe recombination in terms of radiative and Auger recombination.

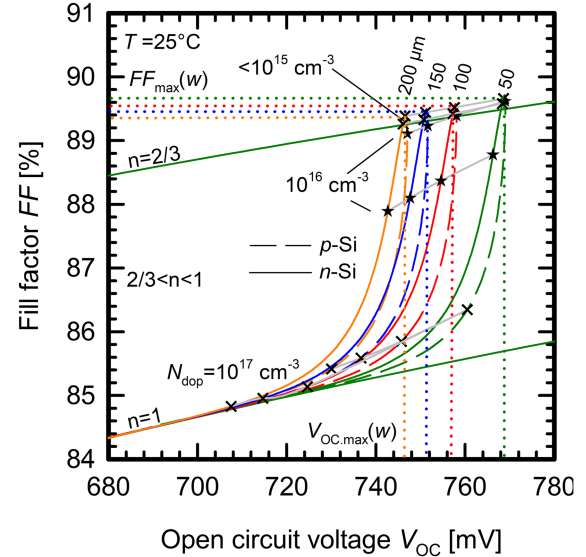


Fig. 2. Colored solid and long dashed curves: FF - V_{OC} dataset calculated by means of analytical simulations of J - V curves of crystalline p- and n-type silicon solar cells with thicknesses 50, 100, 150, and 200 μm and dopant densities varied between 10^{12} and 10^{18} cm^{-3} . Dotted vertical lines: Maximum open-circuit voltage values $V_{OC,\text{max}}(w)$. Dotted horizontal line: Maximum fill factor values $FF_{\text{max}}(w)$. Crosses: Data points belonging to the same dopant density. Green lines: Fill factor limits FF_0 calculated for $n = 1$ and $2/3$, respectively.

For calculating the radiative recombination, we follow Schäfer and Brendel [9] using

$$J_{\text{rad}}(V) = qB_{\text{rel},el}\pi \int A_{\text{bb}} \frac{2c}{\lambda^4} \left[\frac{1}{\exp\left(\frac{hc}{\lambda kT} - \frac{qV}{kT}\right) - 1} - \frac{1}{\exp\left(\frac{hc}{\lambda kT}\right) - 1} \right] d\lambda \quad (7)$$

including photon recycling. $B_{\text{rel},el}$ according to Altermatt [18] is used to account for coulomb enhancement effects.

The Auger recombination current density is calculated from

$$J_{\text{Auger}}(\Delta n) = qw(C_{eeh}g_{eeh}(n^2p - n_0^2p_0) + C_{ehh}g_{ehh}(np^2 - n_0p_0^2)) \quad (8)$$

where $n = n_0 + \Delta n$ and $p = p_0 + \Delta p$. The Auger coefficients C and enhancement factors g are taken from the recent publication by Niewelt et al. [19].

We implemented our modeling in Python and verified it with QUOKKA 3 simulations as well as with the efficiency limits provided in [9] and [20]. The results are in agreement with typical numerical deviations.

Fig. 2 shows the intrinsic FF - V_{OC} datasets for p- and n-type silicon deduced from (J - V) curve calculations carried out for various dopant densities N_{dop} between 10^{12} and 10^{18} cm^{-3} and sample thicknesses w of 50, 100, 150, and 200 μm .

For high dopant densities, our data points are in agreement with Green's relation for $n = 1$. This is to be expected since the solar cells are in low injection at such high dopant densities and radiative recombination with $n = 1$ dominates as the intrinsic

TABLE I
PARAMETERS FOR (10) AND (11) TO CALCULATE THE MAXIMUM FF FOR SILICON SOLAR CELLS LIMITED BY INTRINSIC RECOMBINATION

FF	k	l	p	s	t	u	v
n-Si	0.9432	0.0567	57.0	17.0513	0.0083	90.4418	0.00232
p-Si	0.9478	0.0519	76.3	17.3739	0.0093	90.4924	0.00220

recombination pathway. With decreasing dopant density, we see an increasing deviation from the prediction of Green's relation with $n = 1$. This is also to be expected, since with decreasing dopant density, the ratio of Δn to N_{dop} (or Δp to N_{dop} for n-Si) increases significantly. As a result, the fraction of Auger recombination with $n = 2/3$ increases.

For $N_{\text{dop}} < 10^{15} \text{ cm}^{-3}$, Auger recombination dominates completely and we obtain maximum fill factors $FF_{\max}(w)$ slightly above those predicted by Green's relation with $n = 2/3$. This small deviation is a consequence of the most recent Auger parameterization by Richter et al. [20] allowing n values of around 0.65. Moreover, for $N_{\text{dop}} < 10^{15} \text{ cm}^{-3}$, also maximum open-circuit voltages $V_{OC,\max}(w)$ are reached. With sample thickness decreasing from 200 to 50 μm , $V_{OC,\max}$ increases significantly by more than 20 mV from 746.7 to 768.3 mV.

It is essential to understand that each point on the curves in Fig. 2 represents the upper FF and V_{OC} bound for one specific dopant density N_{dop} . This means that the curves in Fig. 2 cannot be used to determine the maximum possible FF for a given V_{OC} . An upper bound calculation always has to be performed for a specific w and N_{dop} .

Moreover, it must be said that the FF -limit of today's solar cells with typical dopant densities below $5 \times 10^{15} \text{ cm}^{-3}$ is essentially independent of N_{dop} and is described by $FF_{\max}(w)$ providing values close to Green's FF_0 -curve with $n = 2/3$. In addition, the V_{OC} -limit for these cells is essentially independent of N_{dop} and defined by $V_{OC,\max}(w)$.

III. PARAMETERIZATION

Analytical solar cell simulations require an extensive understanding and knowledge of the numerous models and parameterizations they are based on. Consequently, parameterizations to calculate upper bounds for FF and V_{OC} as a function of N_{dop} and w would be helpful for a simple evaluation of solar cell results. Such a parameterization can be written for both FF and V_{OC} with the same mathematical relation

$$FF = FF_{\max} \left[k + \frac{l}{1 + \left(\frac{\log(N_{\text{dop}}/\text{cm}^{-3})}{s(w/\mu\text{m})^{-t}} \right)^p} \right] \quad (9)$$

with

$$FF_{\max}/\% = u(w/\mu\text{m})^{-v} \quad (10)$$

and the parameters given in Table I

$$V_{OC} = V_{OC,\max} \left[\kappa + \frac{\lambda}{1 + \left(\frac{\log(N_{\text{dop}}/\text{cm}^{-3})}{\sigma(w/\mu\text{m})^{-\tau}} \right)^\pi} \right] \quad (11)$$

TABLE II
PARAMETERS REQUIRED IN (12) AND (13) TO CALCULATE THE MAXIMUM V_{OC} FOR SILICON SOLAR CELLS LIMITED BY INTRINSIC RECOMBINATION ONLY

V_{OC}	κ	λ	π	σ	τ	v	φ
n-Si	0.8874	0.1127	49.7	17.86	0.0089	832.8	0.0206
p-Si	0.9100	0.0900	66.0	18.23	0.0106	832.8	0.0206

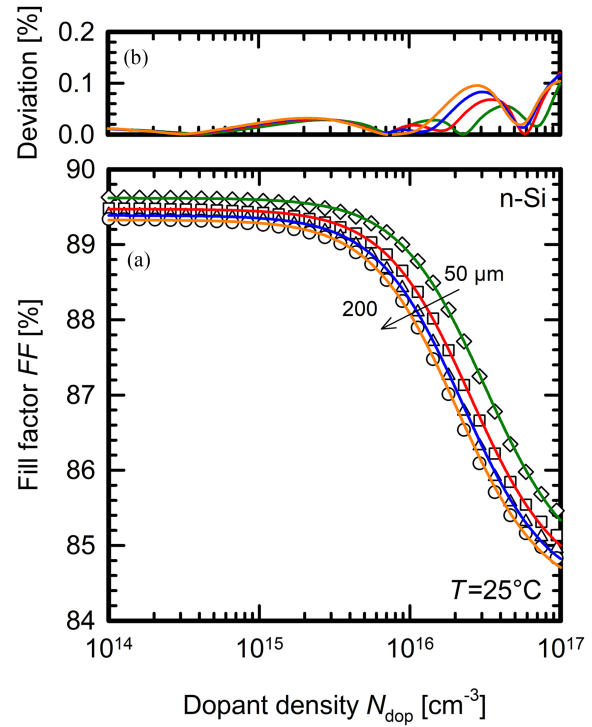


Fig. 3. (a) FF as a function of N_{dop} for n-Si and sample thicknesses of 50, 100, 150, and 200 μm . While symbols are provided by analytical solar cell simulations, lines are calculated by the parameterization given in (9). (b) Deviation between analytical calculation and parameterization. Note that for a sufficiently good approximation, the parameterization should only be used for $N_{\text{dop}} \leq 10^{17} \text{ cm}^{-3}$.

with

$$V_{OC,\max}/mV = v(w/\mu\text{m})^{-\varphi} \quad (12)$$

and the parameters given in Table II.

Figs. 3(a) and 4(a) show the parameterizations for FF and V_{OC} for n-Si compared with the analytically computed values (plots for p-Si are shown in the Appendix). In addition, Figs. 3(b) and 4(b) show their percentage difference. Note that (9) and (11) provide a sufficiently good agreement with the analytical values only for $N_{\text{dop}} \leq 10^{17} \text{ cm}^{-3}$ resulting in a maximum FF deviation of 0.12%_{rel} and a maximum V_{OC} deviation of 0.32%_{rel}.

Figs. 3(a) and 4(a) show that both FF and V_{OC} increase with decreasing N_{dop} until reaching plateaus for $N_{\text{dop}} < 10^{15} \text{ cm}^{-3}$. These plateaus indicate that the intrinsic limits become independent of N_{dop} and only depend on the sample thickness w . Consequently, for $N_{\text{dop}} < 10^{15} \text{ cm}^{-3}$, (10) and (12) are sufficient to calculate upper bounds for today's solar cell even though (9) and (11) give slightly more precise values.

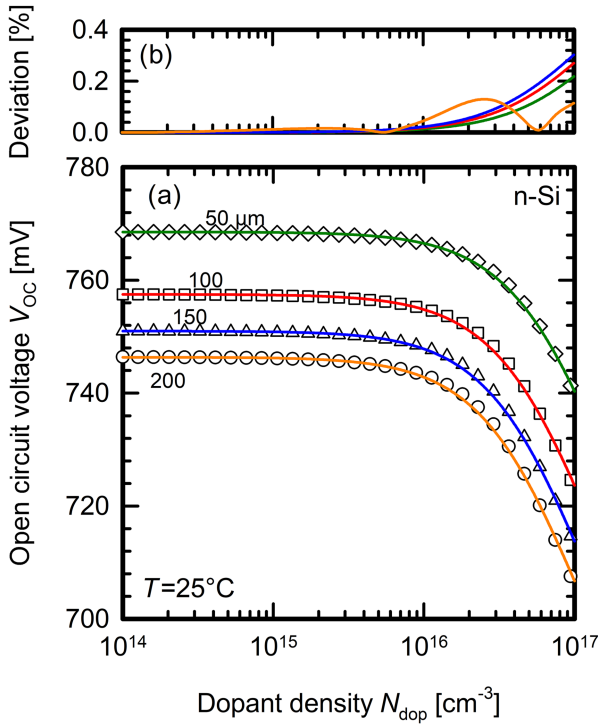


Fig. 4. (a) V_{OC} as a function of N_{dop} for n-Si and sample thicknesses of 50, 100, 150, and 200 μm . While symbols are provided by analytical solar cell simulations, lines are calculated by the parameterization given in (11). (b) Deviation between analytical calculations and parameterization. Note that for a sufficiently good approximation, the parameterization should only be used for $N_{dop} \leq 10^{17} \text{ cm}^{-3}$.

IV. IMPACT OF ADDITIONAL RECOMBINATION AND RESISTANCE EFFECTS

Although the main goal of this work is to calculate upper bounds for FF and V_{OC} , the question naturally arises as to what influence additional recombination and series resistances have on these bounds. To account for additional recombination, we added the term

$$J_{\text{rec.add}} = \frac{J_{0,\text{add}} \Delta n (N_{dop} + \Delta n)}{n_{i0}^2} \quad (13)$$

to J_{rec} in (2). For $N_{dop} = 10^{15} \text{ cm}^{-3}$ and $w = 150 \mu\text{m}$, the dashed line in Fig. 5 shows the impact of this additional recombination path by varying $J_{0,\text{add}}$ between 0 and 100 fA/cm². The series resistance R_s is taken into account as an external resistance (not impacting on the diode voltage V) by relating final J values to V' instead of V , where V' is calculated according to $V' = V - JR_s$ with V calculated with (5).

The solid blue line is included for reference purposes and shows the possible $FF-V_{OC}$ pairs as a function of the base dopant density varied between 10^{12} and 10^{18} cm^{-3} (same data as the blue line in Fig. 2).

Comparing these two curves, it becomes clear that the solid blue line does not represent a universal $FF-V_{OC}$ limit. For example, a 10^{15} cm^{-3} doped solar cell with an additional recombination of 10 fA/cm² has a V_{OC} limit of 732.6 mV and an FF limit of 86.4%. The blue solid line would only allow an

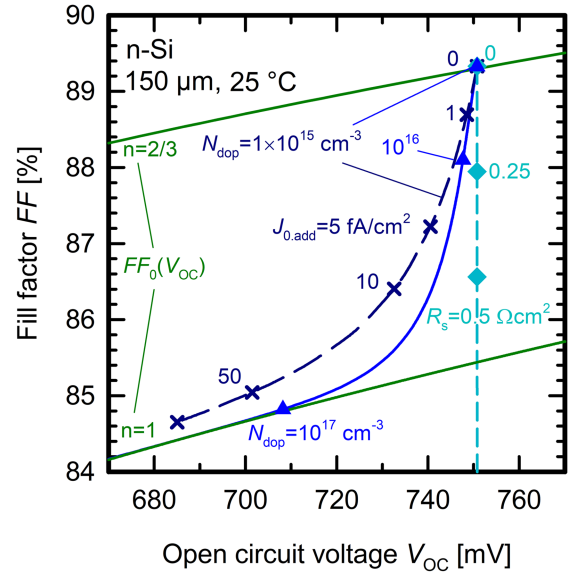


Fig. 5. Solid blue line: $FF-V_{OC}$ data points for various dopant densities varied between 10^{12} and 10^{18} cm^{-3} (same data as solid blue line in Fig. 2). Dashed dark blue and cyan lines: Impact of additional recombination expressed by a $J_{0,\text{add}}$ varied between 0 and 100 fA/cm² as well as impact of a series resistance varied between 0 and $1 \Omega\cdot\text{cm}^2$ on the upper bounds of V_{OC} and FF for 150- μm -thick n-type Si solar cell with a base dopant density of $1 \times 10^{15} \text{ cm}^{-3}$. Green lines: Fill factor limits FF_0 calculated for $n = 1$ and $2/3$, respectively.

FF of 85.6% for this voltage. However, this data pair belongs to a dopant density of $2.9 \times 10^{16} \text{ cm}^{-3}$ and not $1 \times 10^{15} \text{ cm}^{-3}$. Thus, disregarding the dopant density when calculating FF and V_{OC} upper bounds leads to wrong assumptions.

As a short dashed cyan line, Fig. 5 shows the impact of a series resistance, which only impacts on the FF but not on V_{OC} . Already a small R_s of $0.25 \Omega\cdot\text{cm}^2$ reduces the FF limit by 1.2%_{abs}.

V. EVALUATION OF RECORD VALUES

Finally, we have to answer the question whether the reported $FF-V_{OC}$ pairs, as shown in Fig. 1, as crosses are in agreement with the upper FF and V_{OC} bounds calculated for intrinsic recombination. In Fig. 6, we only show data points for n-type silicon solar cells. All gray crosses belong to the data reported in the solar cell efficiency tables. For the cell with the highest V_{OC} , we have exemplarily plotted the associated measurement uncertainties for both parameters.

For the data points also marked by red crosses, Lin et al. [21] state a thickness of approximately 130 μm and a dopant density of around $N_{dop} = 3 \times 10^{15} \text{ cm}^{-3}$. The black star marks the related upper FF and V_{OC} bounds of 752.6 mV and 89.2%, respectively. As required, all red crosses are below these upper limits. Since Lin et al. also provide information about the series resistance and the surface recombination of these cells, we can also take this into account in our simulations. The black triangle represents the upper bounds when calculating with a series resistance of $0.2 \Omega\text{cm}$ as well as with an additional recombination of 1 fA/cm^2 . Even these stricter limits are not violated.

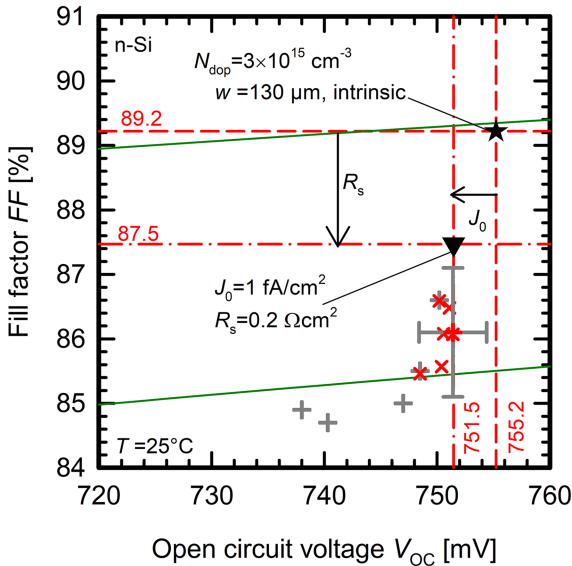


Fig. 6. Gray crosses indicate $FF-V_{OC}$ pairs of n-type silicon solar cells published in the solar cell efficiency tables. Exemplarily, the typical measurement uncertainties of a calibration measurement are shown for the sample with highest V_{OC} . For the red crosses, Lin et al. [21] state a thickness of $130 \mu\text{m}$ and a base dopant density of $3 \times 10^{15} \text{ cm}^{-3}$. The black star marks the corresponding intrinsic upper limits for FF and V_{OC} below which all red crosses lie. Even the more strict limits, indicated by the black triangle, resulting from additional recombination and a series resistance, as stated in [21], are not violated.

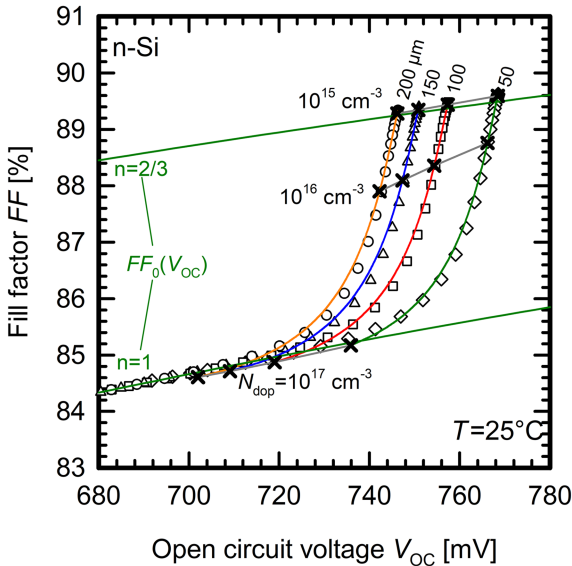


Fig. 7. $FF-V_{OC}$ dependence as determined from analytical solar cell simulations (symbols) as well as provided by the combination of the parameterizations, as shown in Figs. 3(a) and 4(a) (lines). Black crosses mark data points related to dopant densities of 10^{15} , 10^{16} , and 10^{17} cm^{-3} . Green lines: Fill factor limits FF_0 calculated for $n = 1$ and $2/3$, respectively.

VI. SUMMARY

Due to the continuous reduction of carrier recombination in the volume and at the surfaces of crystalline silicon solar cells, we have observed a clear trend toward higher V_{OC} and FF values in recent years. This trend has led to $FF-V_{OC}$ pairs well above the limit predicted by Green's empirical FF_0 relation for a diode ideality factor of $n = 1$. To show that the published values are physically plausible and not a result of artificially

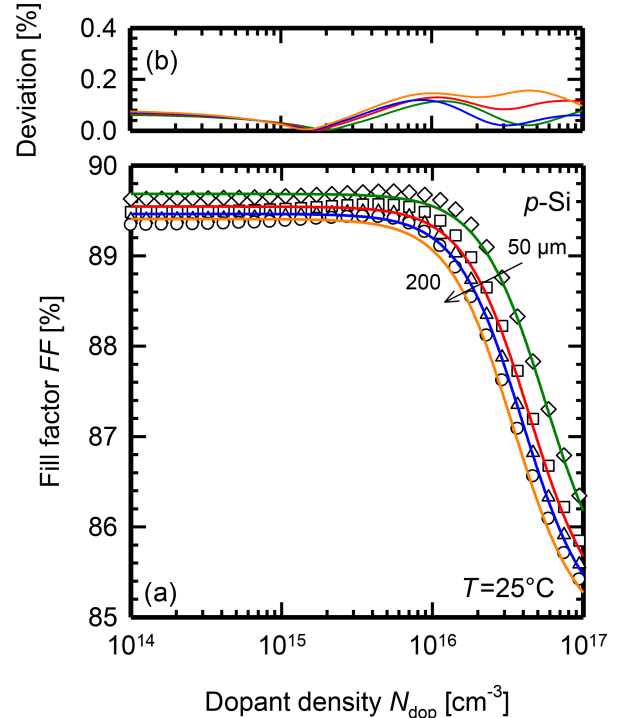


Fig. 8. (a) FF as a function of N_{dop} for p-Si and sample thicknesses of 50, 100, 150, and 200 μm . While symbols are provided by analytical solar cell simulations, lines are calculated by the parameterization given in (10). (b) Deviation between analytical calculation and parameterization. Note that for a sufficiently good approximation, the parameterization should only be used for $N_{dop} \leq 10^{17} \text{ cm}^{-3}$.

overestimating measurements, we have analytically calculated upper FF and V_{OC} bounds for ideal silicon solar cells limited by intrinsic recombination only. With decreasing dopant density, we see a strong increase in the upper FF and V_{OC} bounds until they saturate for dopant densities below 10^{15} cm^{-3} . Consequently, upper bounds can, thus, be calculated by simple $FF_{max}(w)$ and $V_{OC,max}(w)$ parameterizations only depending on the sample thickness.

The $FF_{max}(w)$ values are consistent with values calculated by Green's empirical FF_0 relation using an ideality factor of $n = 2/3$. Based on our calculation, we show that the recently published FF and V_{OC} recorded values do not violate the intrinsic upper limit when correctly considering their dopant density and thickness. Their low base dopant density in combination with a strongly reduced extrinsic recombination results in high injection operation conditions and, consequently, in a limitation by Auger recombination associated with an ideality factor below 1. Thus, a violation of the prediction by Green's empirical FF_0 relation with $n = 1$ is rather to be expected and not a cause for concern.

APPENDIX

From the data, as shown in Figs. 3(a) and 4(a), we can also generate the $FF(V_{OC})$ plot, as shown in Fig. 7, demonstrating how well our parametrization approximates the analytically computed $FF-V_{OC}$ dataset.

For the sake of completeness, Figs. 8 and 9 show the FF and V_{OC} data calculated analytically (symbols) and determined by

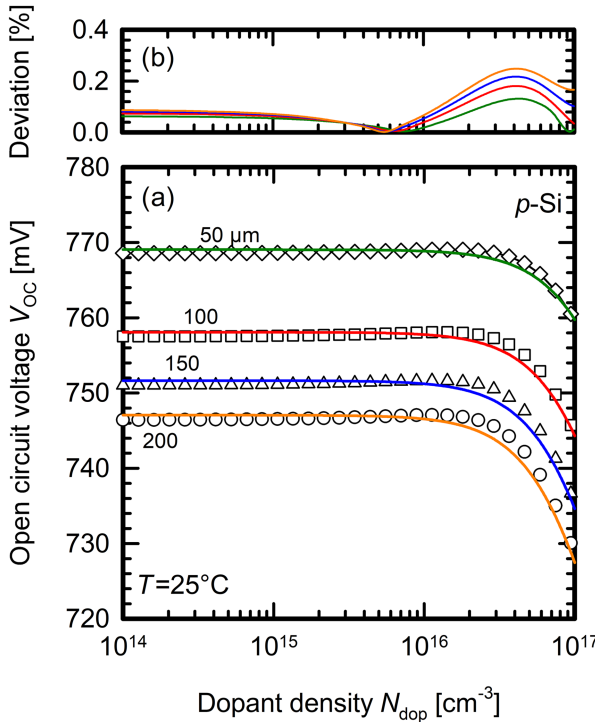


Fig. 9. (a) V_{oc} as a function of N_{dop} for p-Si and sample thicknesses of 50, 100, 150, and 200 μm . While symbols are provided by analytical solar cell simulations, lines are calculated by the parameterization given in (12). (b) Deviation between analytical calculations and parameterization. Note that for a sufficiently good approximation, the parameterization should only be used for $N_{dop} \leq 10^{17} \text{ cm}^{-3}$.

our parameterization (lines) as a function of base dopant density and thickness for p-type silicon solar cells.

ACKNOWLEDGMENT

The discussion with Jan Schmidt about the parameterization of Auger recombination and the resulting limitations for solar cells is greatly acknowledged.

REFERENCES

- [1] J. Schmidt, R. Peibst, and R. Brendel, "Surface passivation of crystalline silicon solar cells: Present and future," *Sol. Energy Mater. Sol. Cells*, vol. 187, pp. 39–54, 2018.
- [2] T. G. Allen, J. Bullock, X. Yang, A. Javey, and S. De Wolf, "Passivating contacts for crystalline silicon solar cells," *Nature Energy*, vol. 4, no. 11, pp. 914–928, Nov. 2019.
- [3] M. A. Green et al., "Solar cell efficiency tables (version 59)," *Prog. Photovolt. Res. Appl.*, vol. 30, no. 1, pp. 3–12, 2022.
- [4] M. A. Green, "Solar cell fill factors: General graph and empirical expression," *Solid State Electron.*, vol. 24, pp. 788–789, 1981.
- [5] M. A. Green, "Accuracy of analytical expressions for solar cell fill factors," *Sol. Cells*, vol. 7, no. 3, pp. 337–340, Dec. 1982.
- [6] C. N. Kruse et al., "Impact of contacting geometries when measuring fill factors of solar cell current–voltage characteristics," *IEEE J. Photovolt.*, vol. 7, no. 3, pp. 747–754, May 2017.
- [7] C. N. Kruse et al., "Impact of contacting geometries on measured fill factors," *Energy Procedia*, vol. 124, pp. 84–90, 2017.
- [8] J. Hohl-Ebinger, D. Grote, B. Hund, A. Mette, and W. Warta, "Contacting bare solar cells for STC measurements," in *Proc. 23rd Eur. Photovolt. Sol. Energy Conf. Exhib.*, 2008, pp. 2012–2016.
- [9] S. Schäfer and R. Brendel, "Accurate calculation of the absorptance enhances efficiency limit of crystalline silicon solar cells with Lambertian light trapping," *IEEE J. Photovolt.*, vol. 8, no. 4, pp. 1156–1158, Jul. 2018.
- [10] M. Rüdiger, J. Greulich, A. Richter, and M. Hermle, "Parameterization of free carrier absorption in highly doped silicon for solar cells," *IEEE Trans. Electron Devices*, vol. 60, no. 7, pp. 2156–2163, Jul. 2013.
- [11] R. Brendel, *Thin-Film Crystalline Silicon Solar Cells: Physics and Technology*. Hoboken, NJ, USA: Wiley, 2003, pp. 16–19.
- [12] M. A. Green, "Improved silicon optical parameters at 25°C, 295 K and 300 K including temperature coefficients," *Prog. Photovolt., Res. Appl.*, vol. 30, no. 2, pp. 164–179, 2022.
- [13] M. A. Green, "Corrigendum to 'improved silicon optical parameters at 25°C, 295K and 300K including temperature coefficients,'" *Prog. Photovolt., Res. Appl.*, vol. 30, no. 9, pp. 1144–1145, Sep. 2022.
- [14] R. Couderc, M. Amara, and M. Lemiti, "Reassessment of the intrinsic carrier density temperature dependence in crystalline silicon," *J. Appl. Phys.*, vol. 115, no. 9, 2014, Art. no. 093705.
- [15] R. Pässler, "Dispersion-related description of temperature dependencies of band gaps in semiconductors," *Phys. Rev. B*, vol. 66, no. 8, 2002, Art. no. 085201.
- [16] P. P. Altermatt, A. Schenk, F. Geelhaar, and G. Heiser, "Reassessment of the intrinsic carrier density in crystalline silicon in view of band-gap narrowing," *J. Appl. Phys.*, vol. 93, pp. 1598–1604, 2003.
- [17] A. Schenk, "Finite-temperature full random-phase approximation model of band gap narrowing for silicon device simulation," *J. Appl. Phys.*, vol. 84, no. 7, pp. 3684–3695, 1998.
- [18] P. P. Altermatt et al., "Injection dependence of spontaneous radiative recombination in crystalline silicon: Experimental verification and theoretical analysis," *Appl. Phys. Lett.*, vol. 88, no. 26, 2006, Art. no. 261901.
- [19] T. Niewelt et al., "Reassessment of the intrinsic bulk recombination in crystalline silicon," *Sol. Energy Mater. Sol. Cells*, vol. 235, 2022, Art. no. 111467.
- [20] A. Richter, M. Hermle, and S. W. Glunz, "Reassessment of the limiting efficiency for crystalline silicon solar cells," *IEEE J. Photovolt.*, vol. 3, no. 4, pp. 1184–1191, Oct. 2013.
- [21] H. Lin et al., "Silicon heterojunction solar cells with up to 26.81% efficiency achieved by electrically optimized nanocrystalline-silicon hole contact layers," *Nature Energy*, vol. 8, pp. 789–799, 2023, doi: [10.1038/s41560-023-01255-2](https://doi.org/10.1038/s41560-023-01255-2).